Magnetic excitations in semiconductor superlattices

Murielle Villeret and S. Rodriguez
Department of Physics, Purdue University, West Lafayette, Indiana 47907

E. Kartheuser
Institut de Physique, Université de Liège, B-4000 Liège, Belgium
(Received 20 April 1988; revised manuscript received 18 July 1988)

We present a theoretical study of magnetostatic excitations in ferromagnetic and antiferromagnetic films and in superlattices composed of alternating layers of such materials with paramagnetic and nonmagnetic substances. The motivation for this study is the possibility of observation of these modes of motion in slabs and superlattices of diluted magnetic semiconductors by inelastic light scattering. We classify the excitations in films as "bulklike" and "surfacelike." Periodic excitations propagating along the growth axis of a superlattice occur which can be classified as "pure bulk" modes if the magnetization of the media behaves sinusoidally in each layer; as "pure interface" modes if they propagate along the boundary separating adjacent layers while their amplitudes decay exponentially within each medium and as "bulk-interface" modes when a behavior occurs having "bulk" character in one medium and "surface" character in the other. We give an analysis of the dispersion relations of these modes and the ranges within which their frequencies lie.

I. INTRODUCTION

In addition to the ordinary spin-wave excitations in bulk magnetic crystals there also exist surface modes of magnetization in finite structures. The amplitude of these excitations decays exponentially from the surface of the material toward the interior. Damon and Eshbach[1] have studied such modes in ferromagnetic slabs in the magnetostatic limit. Since their work appeared, considerable interest in surface magnetostatic modes has been stimulated by the possibility of fabricating superlattices formed by alternating layers of two different magnetic materials. Camley, Rahman, and Mills[2] and Grünberg and Mika[3] investigated the spin-wave spectra of semi-infinite and infinite stacks of ferromagnetic slabs magnetized at right angles to the growth axis and separated by nonmagnetic gaps. This work was extended by Camley and Cottam[4] to slabs of antiferromagnetic materials separated by nonmagnetic gaps and to ferromagnetic-nonmagnetic superlattices when the magnetization lies along the axis of the structure.

These studies are directly applicable to metallic magnetic structures. These collective excitations have been observed in the Brillouin spectra due to magnons in Mo/Ni superlattices by Grimsditch *et al.*[5] and by Schuller and Grimsditch.[6] In this paper we focus on excitations which are significant for magnetic semiconductors. In order to provide appropriate background, we review some of the properties of these materials. We study spin waves in diluted magnetic semiconductors (DMS's). The properties of these materials have been reviewed by Furdyna.[7–10]

A typical example of a DMS is $Cd_{1-x}Mn_xTe$ which can form homogeneous solid solutions for Mn atomic concentrations, x, ranging from 0 to 0.75. $Cd_{1-x}Mn_xTe$ crystallizes in the zinc-blende structure for $0 \leq x \leq 0.75$ in which, at random cation sites, Cd is replaced by Mn atoms. For $x < 0.17$, $Cd_{1-x}Mn_xTe$ is paramagnetic for all temperatures. If $x > 0.17$ there is a magnetically ordered phase due to antiferromagnetic coupling between neighboring Mn^{2+} ions below a critical temperature $T_c(x)$. For example, $Cd_{1-x}Mn_xTe$ with $x = 0.75$ is in an antiferromagnetic phase below 40 K. The magnetic excitations of these materials can be investigated using Raman scattering.[11,12] These investigations constitute the motivation for this work.

A Raman scattering study in superlattices of diluted magnetic semiconductors was carried out by Suh *et al.*[13] That work was concerned with scattering by acoustic and optical phonons as well as by magnetic excitations. Only the paramagnetic spin-flip excitation was observed even at liquid-He temperatures in a superlattice composed of alternating layers of $Cd_{0.89}Mn_{0.11}Te$ and $Cd_{0.50}Mn_{0.50}Te$ in which one of the components is expected to exhibit a magnetically ordered phase. This was taken as an indication that the magnetically ordered phase had not been attained.

One of the purposes of this paper is to investigate the nature of the magnetostatic modes in superlattices of magnetic semiconductors such as those of Ref. 13. We discuss the possible magnetic excitations in the cases in which the applied magnetic field $\mathbf{H}_0$ is either parallel to or perpendicular to the axis of the superlattice $\hat{z}$. The sample is assumed to be formed by a series of alternating layers of antiferromagnetic material separated by paramagnetic or nonmagnetic gaps. For simplicity we take the axis of easy magnetization to be parallel to or perpendicular to the growth axis, $\hat{z}$, of the superlattice. In addition, in each case we take $\mathbf{H}_0$ along the axis of magnetization.

In order to understand the nature of the magnetostatic modes in magnetic superlattices, we first study such

modes in ferromagnetic and antiferromagnetic slabs. This is done in Sec. II. We classify the slab modes as "bulk" and "surface" modes depending on whether their amplitudes are periodic or decaying along the normal to the slab. When $\mathbf{H}_0$ is along the normal $\hat{z}$ to the plane surface of the film there are no surface modes while if $\mathbf{H}_0$ is perpendicular to $\hat{z}$ then both bulk and surface excitations are present.

Section III deals with the magnetostatic modes in superlattices following the work of Rodriguez, Camacho, and Quiroga.[14] In Sec. IV we discuss the application to the two cases of superlattices of antiferromagnetic semiconductors separated by gaps of paramagnetic or nonmagnetic materials. We also investigated ferromagnetic-nonmagnetic superlattices.

We classify the magnetostatic modes in these superlattices as: (i) "pure bulk" modes, (ii) "pure interface" modes, and (iii) "bulk-interface" modes. In the first the magnetization is a trigonometric function of the component of the wave vector along the superlattice axis. In the second, the magnetization decays in both types of layers. Finally in the third the modes behave like bulk modes in one type of layer and as surface modes in the other.

II. MAGNETOSTATIC MODES IN FERROMAGNETIC AND ANTIFERROMAGNETIC FILMS

An electromagnetic mode in a magnetic material is said to be magnetostatic if its frequency ν is small compared to v/λ where λ is its wavelength and v its phase velocity. Under such conditions, the relevant Maxwell equations are the equations of magnetostatics, namely $\nabla\times\mathbf{H}=0$, $\nabla\cdot\mathbf{B}=0$, where $\mathbf{H}$ is the intensity of the magnetic field and $\mathbf{B}=\mathbf{H}+4\pi\mathbf{M}$ the magnetic induction. But these fields vary in time because of the precession of the magnetization $\mathbf{M}$ in an external magnetic field.

We take the z axis of a Cartesian coordinate system along the normal to the surface of the film which we suppose to extend to infinity in the x and y directions. The material of the slab is contained in the region $0\le z\le d$, d being its thickness.

The fields $\mathbf{H}$ and $\mathbf{M}$ can be written as sums of time-independent and time-dependent components in the form

$$\mathbf{H}=\mathbf{H}_i+\mathbf{h}e^{-i\omega t} \tag{2.1}$$

and

$$\mathbf{M}=\mathbf{M}_0+\mathbf{m}e^{-i\omega t} . \tag{2.2}$$

Here $\mathbf{h}$ and $\mathbf{b}=\mathbf{h}+4\pi\mathbf{m}$ also obey the equations of magnetostatics and, hence, $\mathbf{h}$ can be derived from a magnetic scalar potential ϕ defined by

$$\mathbf{h}=-\nabla\phi . \tag{2.3}$$

The quantities $\mathbf{H}_i$ and $\mathbf{M}_0$ are the magnetic field inside the slab and the saturation magnetization of the system in this field. The field $\mathbf{H}_i=\mathbf{H}_0+\mathbf{H}_D$ where $\mathbf{H}_0$ and $\mathbf{H}_D$ are the applied and demagnetizing fields, respectively.

In terms of ϕ the magnetostatic equations reduce to

$$-\nabla^2\phi+4\pi\nabla\cdot\mathbf{m}=0 . \tag{2.4}$$

The magnetization $\mathbf{M}$ evolves in time according to the Bloch equation of motion, $\dot{\mathbf{M}}=\gamma\mathbf{M}\times\mathbf{H}$. Keeping only linear time-varying terms,

$$-i\omega\mathbf{m}=\gamma\mathbf{M}_0\times\mathbf{h}+\gamma\mathbf{m}\times\mathbf{H}_i . \tag{2.5}$$

Equation (2.5) can be written as

$$\mathbf{m}=\vec{\chi}\cdot\mathbf{h} , \tag{2.6}$$

where $\vec{\chi}$ is the susceptibility tensor. Outside the film, $\nabla^2\phi=0$ while inside

$$\sum_i(1+4\pi\chi_{ii})\frac{\partial^2\phi}{\partial x_i^2}=-\sum_{i<j}4\pi\chi_{ij}\left[\frac{\partial h_i}{\partial x_j}-\frac{\partial h_j}{\partial x_i}\right]=0 . \tag{2.7}$$

The boundary conditions require the continuity of ϕ and of

$$b_z=-\frac{\partial\phi}{\partial z}-\sum_i 4\pi\chi_{zi}\frac{\partial\phi}{\partial x_i} \tag{2.8}$$

at $z=0$ and $z=d$.

Solutions for the scalar potential of the form

$$\phi=\psi(z)e^{i(q_x x+q_y y)} \tag{2.9}$$

are

$$\psi(z)=\begin{cases}Ae^{iQz}+Be^{-iQz}, & 0\le z\le d ,\\ Ce^{-q_\perp z}, & z>d ,\\ De^{q_\perp z}, & z<0 ,\end{cases} \tag{2.10}$$

where $q_\perp^2=q_x^2+q_y^2$ and

$$Q^2=-[\mu_{xx}q_x^2+\mu_{yy}q_y^2]/\mu_{zz} , \tag{2.11}$$

with $\mu_{ii}=1+4\pi\chi_{ii}$. Application of the boundary conditions shows that waves of the type (2.9) exist when

$$\tan Qd=-2q_\perp Q\mu_{zz}[q_\perp^2-Q^2\mu_{zz}^2+(4\pi)^2(\chi_{zx}q_x+\chi_{zy}q_y)^2]^{-1} . \tag{2.12}$$

We can now classify the magnetic modes according to whether or not their amplitudes decay exponentially along the z direction. If Q is real, the excitation is "bulk-like," while if Q is imaginary ($Q^2<0$), it decreases exponentially along the normal to the film and we call it a "surface wave." Now we consider the cases of ferromagnetic and antiferromagnetic slabs.

A. Ferromagnetic slab

We consider first a ferromagnetic slab and the two cases in which the applied field is perpendicular to and parallel to the surface of the film.

(i) $\mathbf{H}_0$ parallel to $\hat{z}$. Here the nonvanishing components of $\vec{\chi}$ are

$$\chi_{xx}=\chi_{yy}=M_0H_i[H_i^2-(\omega/\gamma)^2]^{-1} \tag{2.13}$$

and

$$\chi_{xy}=-\chi_{yx}=iM_0(\omega/\gamma)[H_i^2-(\omega/\gamma)^2]^{-1}\ . \tag{2.14}$$

The dispersion relation (2.12) for magnetostatic waves becomes

$$\tan Qd=-2Qq_\perp(q_\perp^2-Q^2)^{-1}\ . \tag{2.15}$$

However, from Eqs. (2.11), (2.13), and (2.14)

$$Q^2=-q_\perp^2\mu_{xx}\ . \tag{2.16}$$

The dispersion relation is obtained solving these equations for Q and $q_\perp$ as functions of the angular frequency. Bulklike waves are obtained when Q is real, i.e., when $\mu_{xx}<0$ which requires $H_i<\omega/|\gamma|<\sqrt{H_0H_i}$. The externally applied field H_0 differs from H_i by the demagnetizing field, i.e., $H_i=H_0-4\pi M_0$. For bulklike modes the dispersion relation reads

$$q_\perp d=(-\mu_{xx})^{-1/2}\arctan[-2(-\mu_{xx})^{1/2}(1+\mu_{xx})^{-1}]\ . \tag{2.17}$$

Figures 1 and 2 give the frequency expressed in dimensionless form $\Omega=\omega/4\pi|\gamma|M_0$ as a function of $q_\perp d$ and Qd, respectively. In these graphs we took $H_0=40$ kG and $4\pi M_0=20$ kG. We note that there is an infinity of bulk waves in which the values of $q_\perp d$ for different frequencies differ by integral multiples of $\pi(-\mu_{xx})^{-1/2}$. The corresponding values of Qd differ by integral multiplies of π. We note that $q_\perp d$ tends to zero for all modes in the lower limit of the range of Ω, namely $H_i/4\pi M_0$ (equal to unity in the numerical example shown in Fig. 1). As Ω approaches the upper limit to its range, namely $\sqrt{H_0H_i}/4\pi M_0$, the corresponding values of $q_\perp d$ tend to infinity. There are no surface waves because, if $Q=iQ'$ is purely imaginary, then, Eq. (2.15) implies that

$$\tanh(Q'd)=-2Q'q_\perp(q_\perp^2+Q^{12})^{-1} \tag{2.18}$$

which can have no solution in Q' except $Q'=0$.

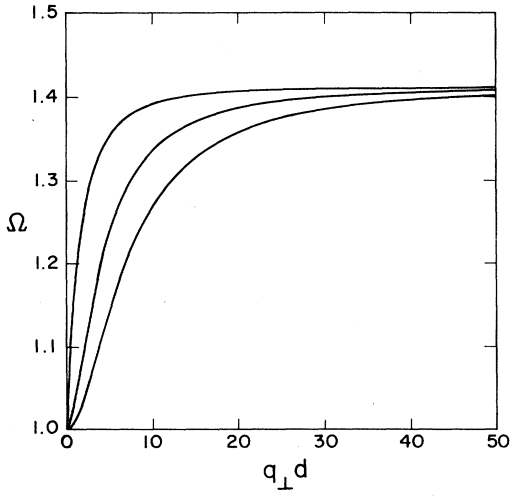

FIG. 1. The reduced frequency $\Omega=\omega/4\pi|\gamma|M_0$ as a function of $q_\perp d$ for "bulklike" waves in a ferromagnetic slab. The external magnetic field, normal to the slab, is taken equal to 40 kG and the saturation magnetization is such that $H_0/4\pi M_0=2$.

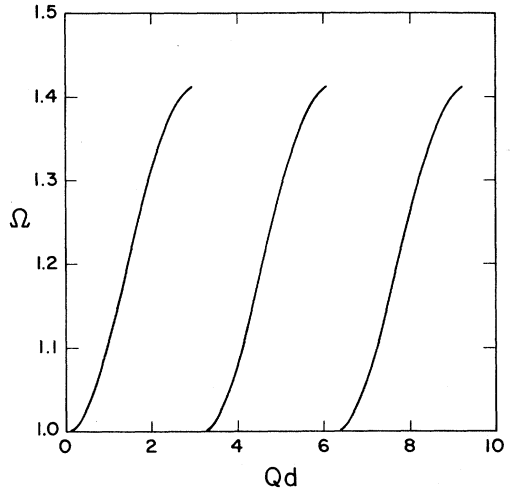

FIG. 2. The reduced frequency Ω for the same situation as in Fig. 1 but as a function of Qd. We note that Ω is periodic in Qd with period π.

(ii) $\mathbf{H}_0$ perpendicular to $\hat{z}$. We take the x axis parallel to $\mathbf{H}_0$ in the plane of the slab. Here the nonvanishing components of $\overleftrightarrow{\chi}$ are

$$\chi_{yy}=\chi_{zz}=M_0H_0[H_0^2-(\omega/\gamma)^2]^{-1} \tag{2.19}$$

and

$$\chi_{yz}=-\chi_{zy}=iM_0(\omega/\gamma)[H_0^2-(\omega/\gamma)^2]^{-1}\ . \tag{2.20}$$

It is convenient to define the frequencies $\omega_1=|\gamma|H_0$ and

$$\omega_2=|\gamma|(H_0B_0)^{1/2}=|\gamma|[H_0(H_0+4\pi M_0)]^{1/2}\ .$$

The latter is the frequency for long wavelengths $2\pi/q_\perp$. The expressions for $\mu_{yy}=1+4\pi\chi_{yy}$ and $4\pi\chi_{zy}$ in terms of these frequencies are

$$\mu_{yy}=-\frac{\omega_2^2-\omega^2}{\omega^2-\omega_1^2} \tag{2.21}$$

and

$$4\pi\chi_{zy}=i\frac{\omega}{\omega_1}\frac{\omega_2^2-\omega_1^2}{\omega^2-\omega_1^2}\ . \tag{2.22}$$

We obtain these expressions from Eqs. (2.5) and (2.6) recalling that in this geometry there is no demagnetizing field parallel to the surface of the slab. The condition for the existence of magnetostatic modes is now

$$\tan Qd=-2\mu_{yy}Qq_\perp[q_\perp^2+(4\pi\chi_{zy}q_y)^2-(\mu_{yy}Q)^2]^{-1} \tag{2.23}$$

with

$$Q^2=-q_y^2-\frac{q_x^2}{\mu_{yy}} . \tag{2.24}$$

We designate by θ the angle between the magnetic field and the direction of propagation of the wave in the plane of the slab, i.e., $q_x=q_\perp\cos\theta$, $q_y=q_\perp\sin\theta$. Then, Eqs. (2.23) and (2.24) are written in the form

$$\tan Qd=-2\mu_{yy}(Q/q_\perp)[\,1+(4\pi\chi_{zy}\sin\theta)^2 -(\mu_{yy}Q/q_\perp)^2]^{-1} \tag{2.25}$$

and

$$(Q/q_\perp)^2=-\sin^2\theta-\mu_{yy}^{-1}\cos^2\theta . \tag{2.26}$$

The frequency range for which propagation at an angle θ takes place is given by the requirement

$$0<-\mu_{yy}<\cot^2\theta \tag{2.27}$$

or

$$\omega_{12}^2(\theta)\equiv\omega_1^2\cos^2\theta+\omega_2^2\sin^2\theta<\omega^2<\omega_2^2 . \tag{2.28}$$

This restriction seems to have been overlooked by previous workers in this field. In Figs. 3 and 4 we show Ω as a function of $q_\perp$ and Q for various choices of the angle θ.

If $Q=iQ'$, $Q'>0$, we obtain the condition for the surface modes, namely,

$$\tanh Q'd=-2\mu_{yy}(Q'/q_\perp)[\,1+(4\pi\chi_{zy}\sin\theta)^2 +(\mu_{yy}Q'/q_\perp)^2]^{-1} , \tag{2.29}$$

and

$$(Q'/q_\perp)^2=\sin^2\theta+\mu_{yy}^{-1}\cos^2\theta . \tag{2.30}$$

These equations can be rewritten in the form

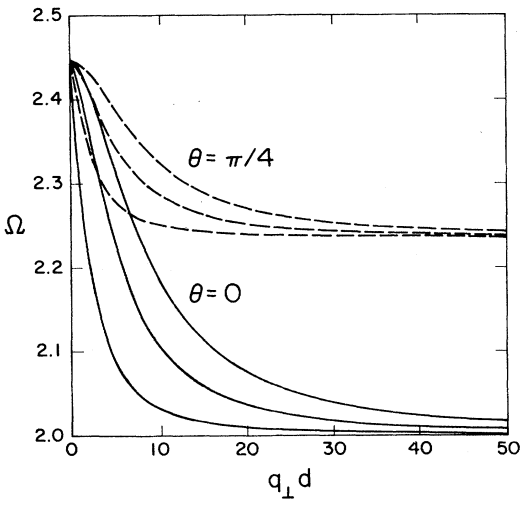

FIG. 3. The reduced frequency Ω as a function of $q_\perp d$ for two values of the angle θ between $\mathbf{H}_0$ and $\mathbf{q}_\perp$. Numerical parameters corresponding to the ferromagnetic slab in Fig. 1. The magnetic field is in the plane of the slab.

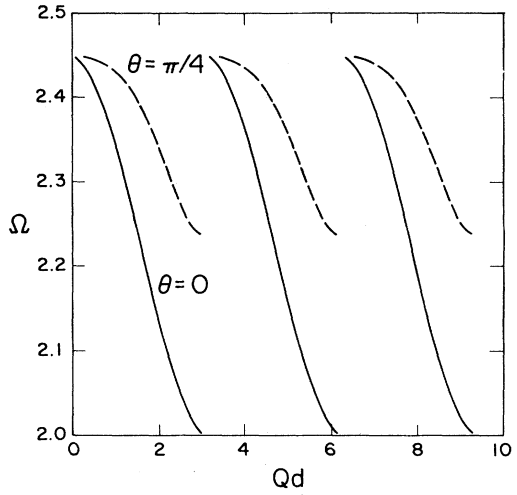

FIG. 4. The reduced frequency Ω for the ferromagnetic slab of Fig. 3 as a function of Qd for $\theta=0$ and $\pi/4$. $\mathbf{H}_0$ in the plane of the slab.

$$\tanh Q'd=(Q'/q_\perp)(\omega_2^2-\omega^2)[\omega^2-\omega^2(\theta)]^{-1} \tag{2.31}$$

and

$$(Q'/q_\perp)^2=[\omega^2-\omega_{12}^2(\theta)](\omega^2-\omega_2^2)^{-1} , \tag{2.32}$$

where

$$\omega^2(\theta)=\tfrac{1}{2}\omega_1^2+\tfrac{1}{2}\omega_2^2\cos^2\theta+(\omega_2^4/2\omega_1^2)\sin^2\theta =\tfrac{1}{2}\omega_1^2+\tfrac{1}{2}(\omega_2/\omega_1)^2\omega_{12}^2(\theta) . \tag{2.33}$$

The conditions for the existence of surface modes propagating on the plane of the slab are that the right-hand

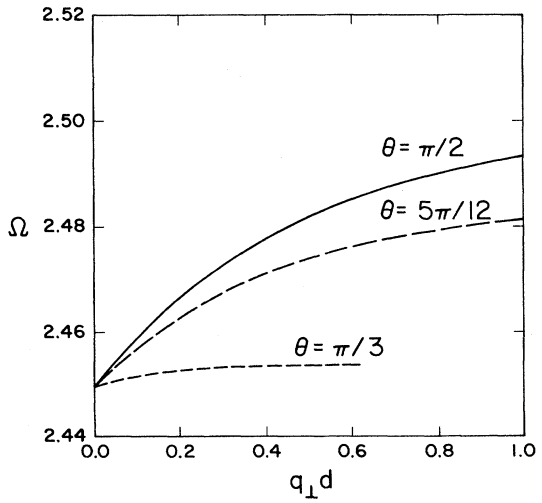

FIG. 5. The reduced frequency as a function of $q_\perp d$ for "surface" waves in a ferromagnetic slab. The parameters are the same as for Figs. 1–4. Three different angles θ between $\mathbf{H}_0$ and $\mathbf{q}_\perp$ have been selected. $\mathbf{H}_0$ in the plane of the slab. Note that no "surface" waves exist for $\theta=0$.

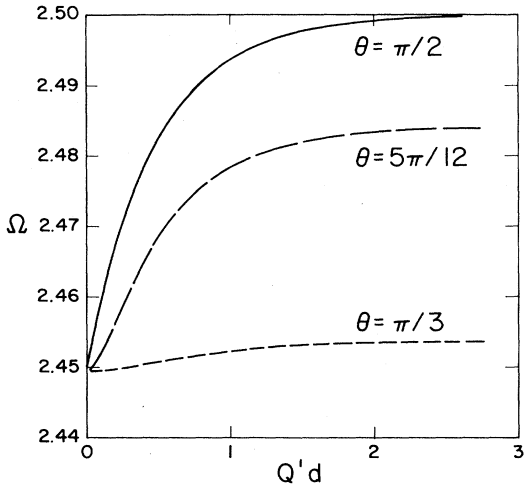

FIG. 6. The reduced frequency as a function of $Q'd$ for the conditions of Fig. 5.

side of Eq. (2.31) lie between 0 and 1 and that of Eq. (2.32) be positive. These requirements are satisfied if (1) $\omega^2-\omega_{12}^2(\theta)$ and $\omega^2-\omega_2^2$ have the same sign, (2) $\omega^2-\omega_2^2$ and $\omega^2-\omega^2(\theta)$ have opposite signs, and (3) $2\omega\omega_1\sin\theta<\omega_1^2+\omega_2^2\sin^2\theta$. For example, for $\theta=0$ there are no surface waves while for $\theta=\pi/2$ there are surface waves propagating on the plane of the slab, for frequencies such that

$$\omega_2<\omega<(\omega_1^2+\omega_2^2)/2\omega_1 . \tag{2.34}$$

For arbitrary angles θ surface waves exist only for $\sin\theta>\omega_1/\omega_2$ and their frequencies are in the range

$$\omega_2<\omega<(\omega_1^2+\omega_2^2\sin^2\theta)/(2\omega_1\sin\theta) . \tag{2.35}$$

No propagating modes exist for $\omega<\omega_2$. Figures 5 and 6 show the reduced frequency of "surface" modes as functions of $q_\perp d$ and Qd, respectively. The calculations are carried out for three different values of θ.

B. Antiferromagnetic slab

In an antiferromagnet the magnetic ions are classified into two classes with opposite preferential orientations. We label them by subindices 1 and 2 so that, e.g., their contributions to the magnetization are $\mathbf{M}_1$ and $\mathbf{M}_2$, respectively. We consider a uniaxial antiferromagnet with an anisotropy field $\mathbf{H}_A$. The equations of motion for these quantities are

$$\frac{\partial\mathbf{M}_{1,2}}{\partial t}=\gamma\mathbf{M}_{1,2}\times(\mathbf{H}-\lambda\mathbf{M}_{2,1}\pm\mathbf{H}_A) , \tag{2.36}$$

where $\lambda\mathbf{M}_1$ ($\lambda\mathbf{M}_2$) is the exchange field due to magnetic ions of type 1 (2) on ions of type 2 (1). For simplicity we shall take the externally applied magnetic field $\mathbf{H}_0$ parallel to $\mathbf{H}_A$. The partial magnetizations are of the form

$$\mathbf{M}_{1,2}=\pm\mathbf{M}_0+\mathbf{m}_{1,2}e^{-i\omega t} , \tag{2.37}$$

where $\mathbf{M}_0$ is parallel to $\mathbf{H}_A$. We neglect demagnetizing fields since $\mathbf{M}=\mathbf{M}_1+\mathbf{M}_2$ is small. Neglecting terms of second order in $\mathbf{m}_i(i=1,2)$ and $\mathbf{h}$, Eqs. (2.36) and (2.1) with $\mathbf{H}_i=\mathbf{H}_0$ yield

$$-i\omega\mathbf{m}_1=\gamma\mathbf{M}_0\times\mathbf{h}-\gamma\mathbf{H}_E\times\mathbf{m}_2 -\gamma(\mathbf{H}_0+\mathbf{H}_E+\mathbf{H}_A)\times\mathbf{m}_1 \tag{2.38}$$

and

$$-i\omega\mathbf{m}_2=-\gamma\mathbf{M}_0\times\mathbf{h}+\gamma\mathbf{H}_E\times\mathbf{m}_1 -\gamma(\mathbf{H}_0-\mathbf{H}_E-\mathbf{H}_A)\times\mathbf{m}_2 , \tag{2.39}$$

where we define the exchange field as $\mathbf{H}_E=\lambda\mathbf{M}_0$. Forming $\mathbf{m}_1\pm\mathbf{m}_2$ with the aid of Eqs. (2.38) and (2.39) and eliminating $\mathbf{m}_1-\mathbf{m}_2$ we obtain the total magnetization

$$\mathbf{m}=\mathbf{m}_1+\mathbf{m}_2=\chi_L\mathbf{h}+\chi_T\hat{\mathbf{H}}_0\times\mathbf{h} , \tag{2.40}$$

where the longitudinal and transverse magnetic susceptibilities χ_L and χ_T are

$$\chi_L=-\frac{2\gamma^2M_0H_A(\omega^2-\omega_+\omega_-)}{(\omega^2-\omega_+^2)(\omega^2-\omega_-^2)} \tag{2.41}$$

and

$$\chi_T=-\frac{4i\omega\gamma^3H_0M_0H_A}{(\omega^2-\omega_+^2)(\omega^2-\omega_-^2)} \tag{2.42}$$

with

$$\omega_\pm=\pm|\gamma|H_0+|\gamma|(H_A^2+2H_AH_E)^{1/2} . \tag{2.43}$$

It is convenient to introduce the angular frequency ω_A defined by

$$\omega_A=|\gamma|(8\pi M_0H_A)^{1/2} , \tag{2.44}$$

and the permeability

$$\mu=1+4\pi\chi_L=\frac{(\omega^2-\sigma_+^2)(\omega^2-\sigma_-^2)}{(\omega^2-\omega_+^2)(\omega^2-\omega_-^2)} , \tag{2.45}$$

where

$$\sigma_\pm^2=\tfrac{1}{2}(\omega_A^2+\omega_+^2+\omega_-^2) \pm\tfrac{1}{2}[\omega_A^4+2\omega_A^2(\omega_+-\omega_-)^2+(\omega_+^2-\omega_-^2)^2]^{1/2} . \tag{2.46}$$

The transverse susceptibility is expressed in a similar way as

$$4\pi\chi_T=\frac{i\omega\omega_A^2(\omega_+-\omega_-)}{(\omega^2-\omega_+^2)(\omega^2-\omega_-^2)} . \tag{2.47}$$

The equations for the scalar magnetic potential and the boundary conditions yield, of course, the results in (2.11) and (2.12) which we now apply to the special cases of $\mathbf{H}_0$ parallel to and perpendicular to the axis of the slab (z axis).

(i) $\mathbf{H}_0$ parallel to $\hat{z}$. In this case $\mu_{zz}=1$, $\mu_{xx}=\mu_{yy}=\mu$ and the only nonvanishing transverse components of the magnetic susceptibility are $\chi_{xy}=-\chi_{yx}=\chi_T$. We find

$$Q^2=-\mu q_\perp^2 \tag{2.48}$$

and

$$\tan Qd = -2Qq_\perp(q_\perp^2 - Q^2)^{-1} . \tag{2.49}$$

Propagating bulk modes exist if

$$\frac{Q^2}{q_\perp^2} = -\frac{(\omega^2-\sigma_+^2)(\omega^2-\sigma_-^2)}{(\omega^2-\omega_+^2)(\omega^2-\omega_-^2)} > 0 . \tag{2.50}$$

Since

$$\omega_- < \sigma_- < \omega_+ < \sigma_+ \tag{2.51}$$

their allowed frequencies occur in the ranges

$$\omega_- < \omega < \sigma_- \tag{2.52}$$

and

$$\omega_+ < \omega < \sigma_+ . \tag{2.53}$$

Figures 7 and 8 show the dispersion of these modes as a function of $q_\perp$ and Q, respectively. The frequency is expressed in the dimensionless form ω/ω_A and we have selected, for convenience, $H_0 = 60$ kG, $H_E = 200$ kG, $H_A = 30$ kG, and $M_0 = 0.2$ kG. These parameters are appropriate for $Cd_{1-x}Mn_xTe$ ($x = 0.7$). We note that we use a theory valid for uniaxial antiferromagnets even in the case of a cubic material. As in the case of a ferromagnetic material there are no surface modes in this geometrical arrangement.

(ii) $\mathbf{H}_0$ perpendicular to $\hat{z}$. This case has been considered by Stamps and Camley.[15] Taking the x axis along $\mathbf{H}_0$, Eq. (2.11) yields

$$(Q/q_\perp)^2 = -\sin^2\theta - \mu^{-1}\cos^2\theta = -\frac{[\omega^2-\sigma_+^2(\theta)][\omega^2-\sigma_-^2(\theta)]}{(\omega^2-\sigma_+^2)(\omega^2-\sigma_-^2)} , \tag{2.54}$$

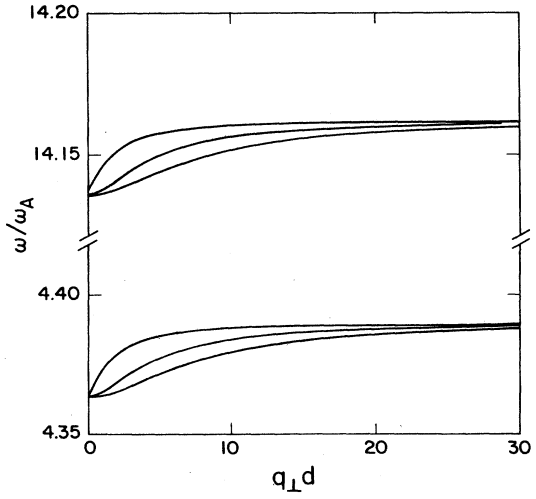

FIG. 7. The frequency ω (expressed in terms of the dimensionless quantity ω/ω_A) as a function of $q_\perp d$ for the antiferromagnetic "bulk" modes. $\mathbf{H}_0$ is normal to the plane of the slab. The following parameters were used: $H_0 = 60$ kG, $H_E = 200$ kG, $H_A = 30$ kG, and $M_0 = 0.2$ kG.

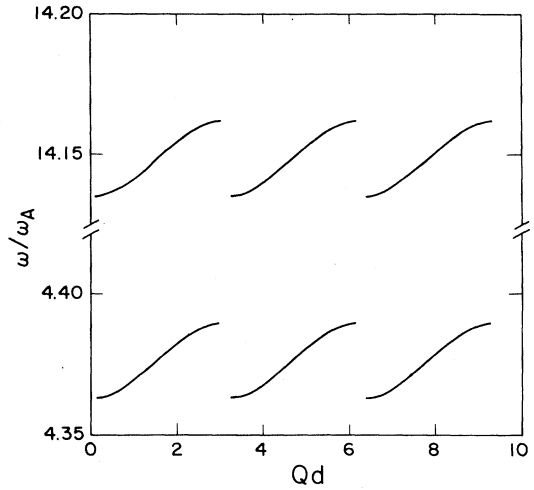

FIG. 8. The frequency ω as a function of Qd under conditions identical to those of Fig. 7.

where

$$\sigma_\pm^2(\theta) = \tfrac{1}{2}(\omega_A^2\sin^2\theta + \omega_+^2 + \omega_-^2) \pm \tfrac{1}{2}[\omega_A^4\sin^4\theta + 2\omega_A^2(\omega_+ - \omega_-)^2\sin^2\theta + (\omega_+^2 - \omega_-^2)^2]^{1/2} . \tag{2.55}$$

Equation (2.12) becomes

$$\tan Qd = -2\mu(Q/q_\perp)[1 + (4\pi\chi_T\sin\theta)^2 - (\mu Q/q_\perp)^2]^{-1} \tag{2.56}$$

after use is made of $\mu_{zz} = \mu_{yy} = \mu$, $\mu_{xx} = 1$, $\chi_{yz} = \chi_T$, and $\chi_{zx} = 0$. The angle formed by $\mathbf{H}_0$ and $\mathbf{q}_\perp$ is denoted by θ.

The condition for the existence of bulk modes is

$$\frac{(\omega^2-\omega_+^2)(\omega^2-\omega_-^2)}{(\omega^2-\sigma_+^2)(\omega^2-\sigma_-^2)} < -\tan^2\theta . \tag{2.57}$$

We note that $\omega_- < \sigma_-(\theta) < \sigma_- < \omega_+ < \sigma_+(\theta) < \sigma_+$ and deduce that the allowed frequencies of these modes are in the ranges $\sigma_-(\theta) < \omega < \sigma_-$ and $\sigma_+(\theta) < \omega < \sigma_+$. The latter two ranges collapse to single values when $\theta = \pi/2$. Figures 9 and 10 show dispersion relations of the bulk modes for four values of θ as functions of $q_\perp d$ and Qd. From Eq. (2.56) we obtain

$$\tan Qd = -\frac{2Q}{q_\perp}\left[1 - \left[\frac{Q}{q_\perp}\right]^2 + \frac{\omega_A^4\sin^2\theta}{(\omega^2-\sigma_+^2)(\omega^2-\sigma_-^2)}\right]^{-1} \tag{2.58}$$

with the aid of Eqs. (2.45) and (2.47).

We can solve Eq. (2.54) for ω^2 as a function of $(Q/q_\perp)^2$ and θ. Substitution of the result thus obtained in Eq. (2.58) yields a transcendental equation connecting Qd and $q_\perp d$ and θ.

We now discuss the special cases in which $\mathbf{H}_0 = \mathbf{0}$ for all angles and of $\mathbf{H}_0 \neq \mathbf{0}$ for $\theta = 0$ or $\pi/2$. If $\mathbf{H}_0 = \mathbf{0}$, then

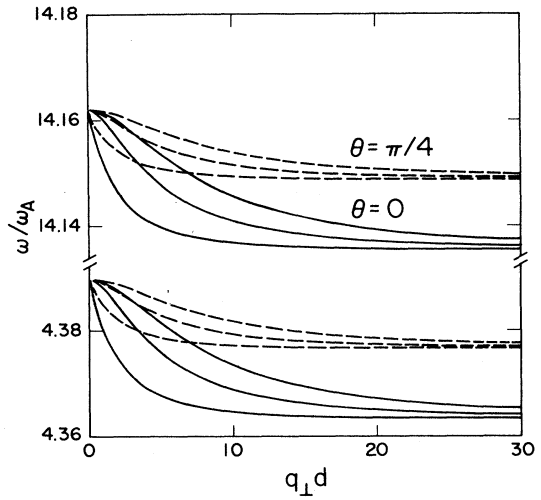

FIG. 9. The frequency of "bulk" modes as a function of $q_\perp d$ for an antiferromagnetic slab. $\mathbf{H}_0$ is in the plane of the slab. Material parameters as in Fig. 7. The angle θ between $\mathbf{H}_0$ and $\mathbf{q}_\perp$ is 0 or $\pi/4$.

$$\omega_+=\omega_-=\omega_M=|\gamma|(H_A^2+2H_AH_E)^{1/2}\ ,$$

the frequency of antiferromagnetic spin waves in the long wavelength limit. Also, in this limit $\sigma_+^2(\theta)=\omega_M^2+\omega_A^2\sin^2\theta$ and $\sigma_-(\theta)=\omega_M$. Equation (2.54) reduces to

$$\left[\frac{Q}{q_\perp}\right]^2=\frac{\omega^2-\omega_M^2-\omega_A^2\sin^2\theta}{\omega_M^2+\omega_A^2-\omega^2}\ . \tag{2.59}$$

This condition restricts the frequency of the allowed bulk modes to the range

$$(\omega_M^2+\omega_A^2\sin^2\theta)^{1/2}\le\omega\le(\omega_M^2+\omega_A^2)^{1/2}\ . \tag{2.60}$$

From Eq. (2.59) we obtain

$$\omega^2=\omega_M^2+\omega_A^2-\omega_A^2[1+(Q/q_\perp)^2]^{-1}\cos^2\theta\ . \tag{2.61}$$

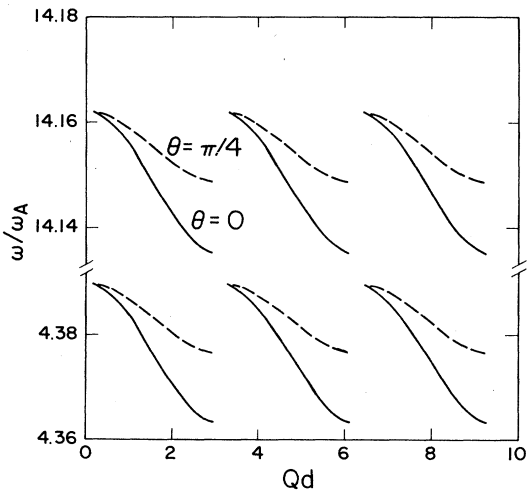

FIG. 10. Same as Fig. 9 but with ω as a function of Qd.

Use of Eqs. (2.58) and (2.59) and of the inequalities (2.60) shows that, given θ and $q_\perp$, we find Q by solving the transcendental equations

$$\tan\frac{Qd}{2}=\frac{Qq_\perp\cos^2\theta}{Q^2+q_\perp^2\sin^2\theta} \tag{2.62}$$

and

$$\tan\frac{Qd}{2}=-\frac{Q^2+q_\perp^2\sin^2\theta}{Qq_\perp\cos^2\theta}\ . \tag{2.63}$$

The solutions of Eqs. (2.62) and (2.63) verify the conditions $0\le\tan(\frac{1}{2}Qd)\le q_\perp/Q$ and $\tan(\frac{1}{2}Qd)\le-(Q/q_\perp)$, respectively. A schematic graphical solution of these equations is shown in Fig. 11. We observe that the solutions become $Qd=n\pi$ (n integer) for large values of Qd and hence, for large n, there are modes of frequency

$$\omega_n^2=\omega_M^2+\omega_A^2-\omega_A^2[1+(n\pi/q_\perp d)^2]^{-1}\cos^2\theta\ . \tag{2.64}$$

For $\mathbf{H}_0\neq\mathbf{0}$ we consider the extreme cases $\theta=0$ and $\theta=\pi/2$. If $\theta=0$ the allowed frequency ranges become $\omega_-<\omega<\sigma_-$ and $\omega_+<\omega<\sigma_+$. The relation between $q_\perp$ and Q is

$$q_\perp/Q=\tan(\tfrac{1}{2}Qd) \tag{2.65}$$

or

$$q_\perp/Q=-\cot(\tfrac{1}{2}Qd)\ , \tag{2.66}$$

where Qd is selected so that the right-hand sides of these equations are positive. The frequencies of the magnetostatic modes are

$$\omega^2=\tfrac{1}{2}\left[\omega_+^2+\omega_-^2+\omega_A^2\cos^2\frac{Qd}{2}\right]\pm\tfrac{1}{2}\left[(\omega_+^2-\omega_-^2)^2+2\omega_A^2(\omega_+-\omega_-)^2\cos^2\frac{Qd}{2}+\omega_A^4\cos^4\frac{Qd}{2}\right]^{1/2}\ , \tag{2.67}$$

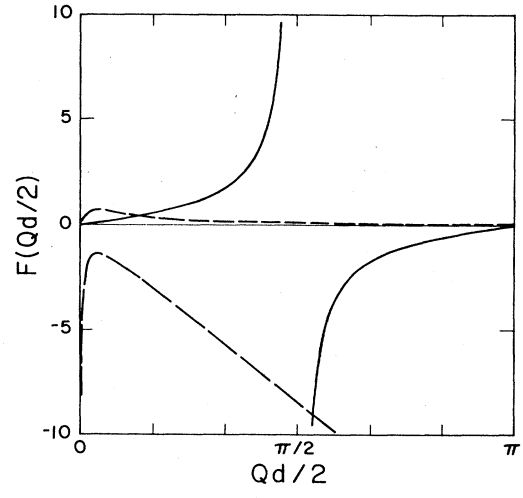

FIG. 11. Graphical solutions of Eqs. (2.62) and (2.63) for $\theta=\pi/6$ and $q_\perp d=0.5$.

when Q is obtained from the solution of Eq. (2.65). If Q is obtained from Eq. (2.66) the expression for ω is the same as in (2.67) except that $\cos(Qd/2)$ is replaced by $\sin(Qd/2)$. Both signs in Eq. (2.67) are allowed since, when $\cos^2(Qd/2)$ and $\sin^2(Qd/2)$ range from 0 to 1, the corresponding frequency intervals are $\omega_- < \omega < \sigma_-$ and $\omega_+ < \omega < \sigma_+$ for the lower and upper signs, respectively. When $\mathbf{H}_0 \neq \mathbf{0}$ and $\theta = \pi/2$, since $\sigma_\pm(\pi/2) = \sigma_\pm$, we find $(Q/q_\perp)^2 = -1$ and there are no bulk modes.

The conditions for the existence of surface modes ($Q = iQ'$) are

$$\left[\frac{Q'}{q_\perp}\right]^2 = \sin^2\theta + \mu^{-1}\cos^2\theta = \frac{[\omega^2-\sigma_+^2(\theta)][\omega^2-\sigma_-^2(\theta)]}{(\omega^2-\sigma_+^2)(\omega^2-\sigma_-^2)} > 0 \tag{2.68}$$

and

$$\tanh Q'd = -\frac{2Q'}{q_\perp}\left[1+\left[\frac{Q'}{q_\perp}\right]^2 + \frac{\omega_A^4\sin^2\theta}{(\omega^2-\sigma_+^2)(\omega^2-\sigma_-^2)}\right]^{-1} . \tag{2.69}$$

These equations require that (1)

$$[\omega^2-\sigma_+^2(\theta)][\omega^2-\sigma_-^2(\theta)]$$

and

$$(\omega^2-\sigma_+^2)(\omega^2-\sigma_-^2)$$

both be negative, and (2)

$$0 \le (\omega^2-\sigma_-^2)(\sigma_+^2-\omega^2)\left[1+\frac{Q'}{q_\perp}\right]^2 \le \omega_A^4\sin^2\theta .$$

The first condition limits the range of allowed frequencies for surface modes to the interval $\sigma_- < \omega < \sigma_+(\theta) < \sigma_+$.

As in the previous case of bulk modes, we now consider the special cases in which $\mathbf{H}_0 = \mathbf{0}$ and θ is arbitrary and $\mathbf{H}_0 \neq \mathbf{0}$ for $\theta = 0$ or $\pi/2$.

When $\mathbf{H}_0 = \mathbf{0}$ Eqs. (2.68) and (2.69) become

$$\left[\frac{Q'}{q_\perp}\right]^2 = \frac{\omega^2-\omega_M^2-\omega_A^2\sin^2\theta}{\omega^2-\omega_M^2-\omega_A^2} \tag{2.70}$$

and

$$\tanh Q'd = -\frac{2Q'}{q_\perp}\frac{(\omega^2-\omega_M^2)(\omega^2-\omega_M^2-\omega_A^2)}{(\omega^2-\omega_M^2)^2+(\omega^2-\omega_M^2-\omega_A^2)(\omega^2-\omega_M^2-\omega_A^2\sin^2\theta)} . \tag{2.71}$$

We note that surface modes can only occur in this case for frequencies ω such that $\omega^2 > \omega_M^2+\omega_A^2$ or $\omega^2 < \omega_M^2+\omega_A^2\sin^2\theta$. If $\omega^2 > \omega_M^2+\omega_A^2$, it follows from Eq. (2.71) that $\tanh Q'd/Q'd$ would be negative and, hence, this range of frequencies is inaccessible to surface modes when $\mathbf{H}_0 = \mathbf{0}$. If $\omega^2 < \omega_M^2+\omega_A^2\sin^2\theta$, $\tanh Q'd/Q'd$ is positive only if $\omega > \omega_M$. Thus, the allowed frequency interval for surface waves in the absence of an externally applied magnetic field is given by $\omega_M < \omega < (\omega_M^2+\omega_A^2\sin^2\theta)^{1/2}$.

Eliminating $Q'/q_\perp$ from Eqs. (2.70) and (2.71) we find four solutions for ω as a function of θ and $Q'd$. However, only two of these are in the allowed frequency range. They are

$$\omega^2 = \omega_M^2+2\omega_A^2\sin^2\theta\{1+\sin^2\theta+[\cos^4\theta+4\sin^2\theta\coth^2(Q'd/2)]^{1/2}\}^{-1} \tag{2.72}$$

and

$$\omega^2 = \omega_M^2+2\omega_A^2\sin^2\theta\{1+\sin^2\theta+[\cos^4\theta+4\sin^2\theta\tanh^2(Q'd/2)]^{1/2}\}^{-1} . \tag{2.73}$$

For example, for very large values of $Q'd$ both branches (2.72) and (2.73) tend to the limit

$$\omega^2 = \omega_M^2+\omega_A^2\sin^2\theta(1+\sin^2\theta)^{-1} . \tag{2.74}$$

When $Q'd = 0$ we find the limits $\omega^2 = \omega_M^2$ and $\omega^2 = \omega_M^2+\omega_A^2\sin^2\theta$. In Fig. 12 we display ω/ω_A as a function of θ for two values of $Q'd$, namely 0.2 and 10.0 for an antiferromagnet whose parameters are those of $Cd_{1-x}Mn_xTe$ ($x = 0.70$). These have already been listed in this paper (see Fig. 7). Figure 13 shows ω/ω_A for the two surface modes as a function of $Q'd$ for various values of θ. We note that when $\theta = 0$, $Q' = 0$ and the resulting motion is indistinguishable from a bulk magnetostatic excitation.

When $\mathbf{H}_0 \neq \mathbf{0}$ and $\theta = \mathbf{0}$,

$$\left[\frac{Q'}{q_\perp}\right]^2 = \frac{(\omega^2-\omega_+^2)(\omega^2-\omega_-^2)}{(\omega^2-\sigma_+^2)(\omega^2-\sigma_-^2)} \tag{2.75}$$

and

$$\tanh Q'd = -2Q'q_\perp(q_\perp^2+Q'^2)^{-1} . \tag{2.76}$$

Thus, these modes only occur when $Q' = 0$ and, clearly, their frequencies are those of the long wavelength antiferromagnetic spin-wave excitations, ω_+ and ω_-.

When $\mathbf{H}_0 \neq \mathbf{0}$ and $\theta = \pi/2$, we find $Q' = q_\perp$ and

$$(\omega^2-\sigma_+^2)(\omega^2-\sigma_-^2) = -(\omega_A^2/2)^2(1-e^{-2q_\perp d}) . \tag{2.77}$$

We conclude that the frequencies of the allowed modes lie in the interval $\sigma_- < \omega < \sigma_+$ and are given by

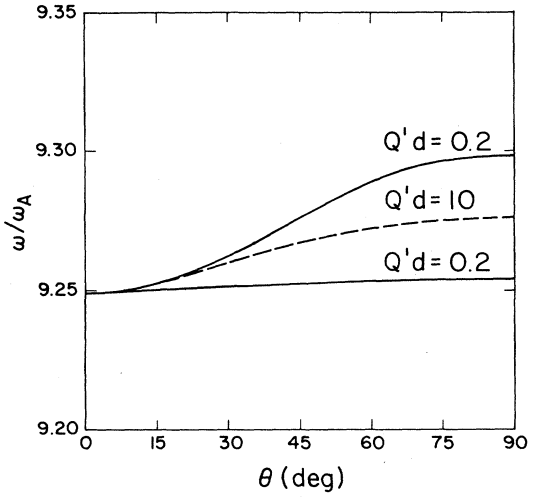

FIG. 12. Frequency of surface modes for an antiferromagnetic slab as a function of θ, the angle between $\mathbf{H}_A$ and $\mathbf{q}_\perp$, when $\mathbf{H}_0=0$ for two values of $Q'd$. Material parameters as in Fig. 7.

$$\omega^2=\tfrac{1}{2}(\omega_+^2+\omega_-^2+\omega_A^2)$$
$$\pm\tfrac{1}{2}[(\omega_+^2-\omega_-^2)^2+2\omega_A^2(\omega_+-\omega_-)^2$$
$$+\omega_A^4 e^{-2q_\perp d}]^{1/2} . \tag{2.78}$$

In particular, when $\mathbf{H}_0=0$, these frequencies are expressed by the relation

$$\omega^2=\omega_M^2+\tfrac{1}{2}\omega_A^2(1\pm e^{-q_\perp d}) . \tag{2.79}$$

Figure 14 shows these frequencies as functions of $q_\perp d$ for $H_0=0$ and $H_0=0.2$ kG for the numerical example mentioned above.

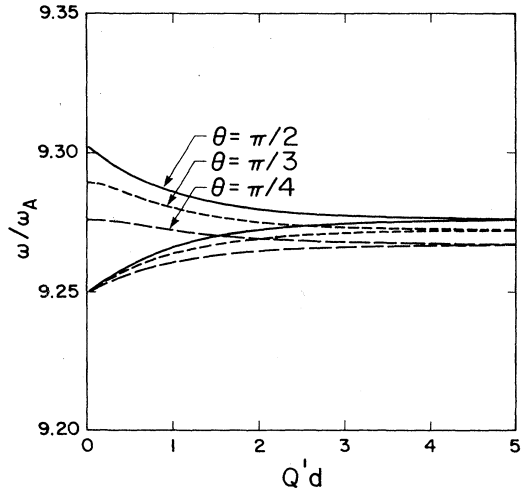

FIG. 13. Frequency of surface modes for an antiferromagnetic slab as a function of $Q'd$ for several values of θ. Parameters and geometrical arrangement as in Fig. 12.

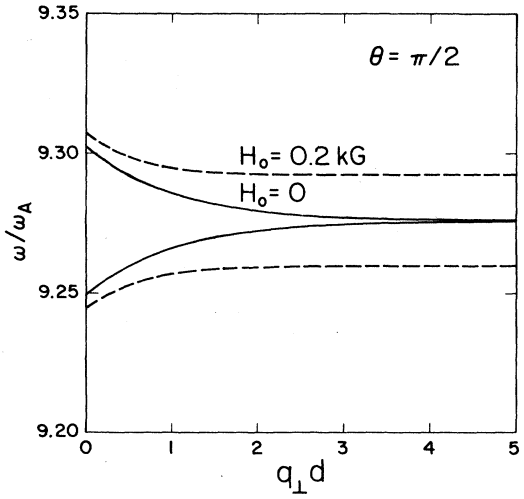

FIG. 14. Frequencies of the surface modes for an antiferromagnetic slab as functions of $q_\perp d$ for $H_0=0$ and 0.2 kG for $\theta=\pi/2$. Parameters and geometrical arrangement as in Fig. 12.

III. MAGNETOSTATIC MODES IN SUPERLATTICES

In this section, we consider a superlattice formed by alternating layers of two magnetic materials which we label by the indices 1 and 2. Their thicknesses are denoted by d_1 and d_2. An example of such a superlattice of the diluted magnetic semiconductor $Cd_{1-x}Mn_xTe$ can be designated by the symbol $Cd_{1-x_1}Mn_{x_1}Te/Cd_{1-x_2}Mn_{x_2}Te$ where x_1 and x_2 are the atomic concentrations of magnetic ions in the layers 1 and 2, respectively. We take a Cartesian coordinate system whose z axis is along the direction of growth of the superlattice.

The equation governing the behavior of the scalar magnetic potential ϕ is given by Eq. (2.7). We must bear in mind that in each layer of the superlattice the quantity $1+4\pi\chi_{ii}$ takes on values characteristic of the material for that particular layer.

The boundary conditions require the continuity of ϕ and of b_z. It is enough to specify the boundary conditions at two successive interfaces and use the Bloch condition

$$\phi(x,y,z+d)=e^{iq_z d}\phi(x,y,z) , \tag{3.1}$$

where

$$d=d_1+d_2 \tag{3.2}$$

is the superperiod along the axis of the superlattice.

The solutions of Eq. (2.7) in our case are of the form

$$\phi_{1,2}(x,y,z)=\{A_{1,2}e^{iQ_{1,2}z}+B_{1,2}e^{-iQ_{1,2}z}\}e^{iq_x x+iq_y y} , \tag{3.3}$$

where the subindices 1 or 2 are for the layers denoted by 1 or 2, respectively. The wave vectors $Q_{1,2}$ are given by

$$Q_{1,2}^2=-(\mu_{xx}^{(1,2)}q_x^2+\mu_{yy}^{(1,2)}q_y^2)/\mu_{zz}^{(1,2)} . \tag{3.4}$$

The boundary conditions applied to Eq. (3.3) and use of

the Bloch theorem (3.1) yield four homogeneous linear equations in A_1, B_1, A_2, and B_2 which have a nontrivial solution only if

$$\cos(q_z d)=\cos(Q_1 d_1)\cos(Q_2 d_2) - f\sin(Q_1 d_1)\sin(Q_2 d_2)\ , \tag{3.5}$$

where

$$f=\{(\mu_{zz}^{(1)}Q_1)^2+(\mu_{zz}^{(2)}Q_2)^2 - 16\pi^2[(\chi_{zx}^{(1)}-\chi_{zx}^{(2)})q_x+(\chi_{zy}^{(1)}-\chi_{zy}^{(2)})q_y]^2\} \times(2\mu_{zz}^{(1)}\mu_{zz}^{(2)}Q_1Q_2)^{-1}\ . \tag{3.6}$$

We consider the cases in which $\mathbf{H}_0$ is directed either parallel to or perpendicular to the axis of the superlattice.

(i) $\mathbf{H}_0$ parallel to $\hat{z}$. In this case $\mu_{zz}^{(1,2)}=1$, $\mu_{xx}^{(1,2)}=\mu_{yy}^{(1,2)}=\mu_{1,2}$, and $\chi_{zx}^{(1,2)}=\chi_{zy}^{(1,2)}=0$. Thus,

$$f=\frac{Q_1^2+Q_2^2}{2Q_1Q_2}\ . \tag{3.7}$$

Equations (3.4) become

$$Q_{1,2}^2=-\mu_{1,2}q_\perp^2\ . \tag{3.8}$$

Four types of modes propagating with real $q_\perp$ can exist depending on the signs of Q_1^2 and Q_2^2. If $Q_{1,2}^2>0$ we have "pure bulk" modes. These occur in the frequency intervals for which both μ_1 and μ_2 are negative. We observe that $f\geq 1$ so that Eq. (3.6) can be written as

$$\cos(q_z d)=\cos(Q_1 d_1+Q_2 d_2) -(f-1)\sin(Q_1 d_1)\sin(Q_2 d_2)\ . \tag{3.9}$$

Since $\cos(q_z d)$ lies between -1 and 1, not all frequencies for which μ_1 and μ_2 are negative need be allowed. If Q_1^2 and Q_2^2 are both negative, denoting $Q_{1,2}=iQ'_{1,2}$, we have

$$\cos(q_z d)=\cosh(Q'_1 d_1)\cosh(Q'_2 d_2) +f\sinh(Q'_1 d_1)\sinh(Q'_2 d_2) \tag{3.10}$$

while $f=(Q_1'^2+Q_2'^2)/2Q'_1Q'_2\geq 1$. No solutions are possible since the right-hand side of Eq. (3.10) exceeds unity. Thus, in this case, no "pure interface" modes exist.

There remains the cases in which Q_1^2 and Q_2^2 are of different signs. Here, we can take, e.g., $Q_1^2>0$ and $Q_2^2<0$. Such modes, which we call "bulk-interface" waves, exist in the frequency ranges in which $\mu_1<0$ and $\mu_2>0$. We write

$$\cos(q_z d)=\cos(Q_1 d_1)\cosh(Q'_2 d_2) -\frac{Q_1^2-Q_2'^2}{2Q_1Q'_2}\sin(Q_1 d_1)\sinh(Q'_2 d_2) \tag{3.11}$$

which may imply an additional restriction on the frequency depending on the value of $q_z d$. The expression for μ_2 is identical to that in Eq. (2.21) except that ω_1 and ω_2 are replaced by $\omega_1'=|\gamma|(H_0-4\pi M_0^{(2)})$ and $\omega_2'=|\gamma|[H_0(H_0-4\pi M_0^{(2)})]^{1/2}$. Here $M_0^{(2)}$ is the magnetization in the paramagnetic regions.

(ii) $\mathbf{H}_0$ parallel to $\hat{x}$. Here we have $\mu_{yy}^{(1,2)}=\mu_{zz}^{(1,2)}=\mu_{1,2}$, $\mu_{xx}=1$, $\chi_{zx}^{(1,2)}=0$, while $\chi_{zy}^{(1,2)}=\chi_{1,2}$. The expression (3.6) becomes

$$f=\frac{\mu_1^2Q_1^2+\mu_2^2Q_2^2-16\pi^2(\chi_1-\chi_2)^2q_y^2}{2\mu_1\mu_2Q_1Q_2} \tag{3.12}$$

and

$$Q_{1,2}^2=-q_y^2-\mu_{1,2}^{-1}q_x^2\ . \tag{3.13}$$

Since we envisage light scattering experiments in which the wave vector $\mathbf{q}_\perp$ is determined by the geometrical arrangement, and since it is difficult to consider general values of $\mathbf{q}_\perp$, we study the cases in which q_x or q_y vanishes.

If $q_x=0$,

$$Q_{1,2}^2=-q_y^2 \tag{3.14}$$

and

$$f=[\mu_1^2+\mu_2^2+16\pi^2(\chi_1-\chi_2)^2]/2\mu_1\mu_2 \tag{3.15}$$

is a function of the frequency alone. We can only have "pure interface" modes. In addition, Eq. (3.5) becomes

$$\cos(q_z d)=\cosh(q_y d_1)\cosh(q_y d_2) +f\sinh(q_y d_1)\sinh(q_y d_2)\ . \tag{3.16}$$

Formula (3.16) is an implicit equation yielding the frequency ω as a function of q_y and q_z. Note that when $f\geq 0$ there are no real solutions for $q_z d$.

When $q_y=0$,

$$Q_{1,2}^2=-q_x^2/\mu_{1,2} \tag{3.17}$$

and

$$f=(\mu_1^2Q_1^2+\mu_2^2Q_2^2)(2\mu_1\mu_2Q_1Q_2)^{-1} =(1+\kappa^2)/2\kappa\ , \tag{3.18}$$

with

$$\kappa=(\mu_1/\mu_2)^{1/2}\ . \tag{3.19}$$

As before the quantity f depends only on the frequency and is real if μ_1 and μ_2 have the same signs, i.e., for "pure bulk" and "pure interface" modes. It is purely imaginary for "bulk-interface" waves.

For the "pure interface" modes we have

$$\cos(q_z d)=\cosh(Q'_1 d_1)\cosh(Q'_2 d_2) +\frac{1+\kappa^2}{2\kappa}\sinh(Q'_1 d_1)\sinh(Q'_2 d_2)$$

which yields no solutions. This is expected since the same behavior was noted for surface modes in a single slab (see Sec. II). In general, such waves exist for an arbitrary angle $\theta=\arctan(q_y/q_x)$. For "bulk-interface" modes, e.g., $\mu_1<0$ and $\mu_2>0$ and $\kappa=i\kappa'=i(|\mu_1|/\mu_2)^{1/2}$, we have

$$\cos(q_z d)=\cos(Q_1 d_1)\cosh(Q'_2 d_2) -\frac{1-\kappa'^2}{2\kappa'}\sin(Q_1 d_1)\sinh(Q'_2 d_2)\ . \tag{3.20}$$

In a similar way, for "pure bulk" modes we obtain

$$\cos(q_z d) = \cos(Q_1 d_1)\cos(Q_2 d_2) - \frac{1+\kappa^2}{2\kappa}\sin(Q_1 d_1)\sin(Q_2 d_2) . \quad (3.21)$$

IV. EXAMPLES OF MAGNETOSTATIC MODES IN SUPERLATTICES

In this section, we consider a few applications of the formalism developed in Sec. III to superlattices composed of different magnetic materials.

A. Antiferromagnetic-paramagnetic superlattices

We consider here the example in which the layers corresponding to the subindex 1 are in an antiferromagnetic phase while those corresponding to 2 are ferromagnetic or paramagnetic. We note that in the latter case the difference between ω_2 and ω_1 is extremely small.

"Pure bulk" modes with $\mathbf{H}_0$ parallel to $\hat{z}$ exist if both μ_1 and μ_2 are negative. These quantities are given by Eqs. (2.45) and (2.21), respectively. Thus, "pure bulk" modes exist only in the region of overlap of the ranges $\omega_1' < \omega < \omega_2', \omega_- < \omega < \sigma_-$ and $\omega_1' < \omega < \omega_2', \omega_+ < \omega < \sigma_+$. The second set of inequalities cannot be satisfied simultaneously while the first is satisfied under rather severe restrictions depending on the intensity of the applied magnetic field. However, since in the paramagnetic phase $\omega_1' \lesssim \omega_2'$, this essentially restricts the allowed modes to those whose frequency is $|\gamma|H_i$, i.e., the paramagnetic excitation. For a sample of $Cd_{0.89}Mn_{0.11}Te$ which is paramagnetic at liquid-helium temperatures we estimate $(\omega_2'/|\gamma|) \approx 59.56$ kG when $(\omega_1'/|\gamma|) = 59.12$ kG. If ω_1' is outside the range $\omega_- < \omega < \sigma_-$ even this mode is forbidden. We note that ω_1' increases with increasing H_0 while ω_- decreases and that ω_1' is in the range $\omega_- < \omega < \sigma_-$ for H_0 larger than $\frac{1}{2}(H_A^2 + 2H_A H_E)^{1/2}$. There exists also an upper limit to H_0 beyond which "pure bulk" modes cannot be present, namely, when $\omega_1' > \sigma_-$. For the parameters used above ($H_0 = 60$ kG, $H_E = 200$ kG, $H_A = 30$ kG, and $M_0 = 0.2$ kG) there are no "pure bulk" modes. However, for other situations they may be present.

"Bulk-interface" modes occur when $\mu_1 < 0$ and $\mu_2 > 0$ and when $\mu_1 > 0$ and $\mu_2 < 0$. In the first case $\omega < \omega_1'$ or $\omega > \omega_2'$, which implies practically no restriction, and $\omega_- < \omega < \sigma_-$ or $\omega_+ < \omega < \sigma_+$. In the second situation we are restricted to the small range $\omega_1' < \omega < \omega_2'$ and we must have either $\omega < \omega_-$, $\sigma_- < \omega < \omega_+$ or $\omega > \sigma_+$. We note that this range is complementary to that of the "pure bulk" modes so that an excitation at approximately the frequency ω_1' is always present. Figure 15 shows the frequency of the "bulk-interface" modes for the parameters used above as a function of $q_z d$ for several values of $q_\perp d_2$. The two branches discussed in the first case above are displayed. We observe that for increasing value of $q_\perp d_2$ the allowed range of $q_z d$ changes. Figure 16 shows the dispersion relation for the second case above in which ω lies in the extremely narrow range $\omega_1' < \omega < \omega_2'$.

We consider now the magnetostatic modes when $\mathbf{H}_0$ is parallel to $\hat{x}$, i.e., perpendicular to the axis of the superlattice. We recall that when $q_x = 0$ we obtain "pure-interface" modes only if $f < 0$. In that case the allowed solutions lie in two extremely narrow ranges of frequency for the numerical example considered here. When

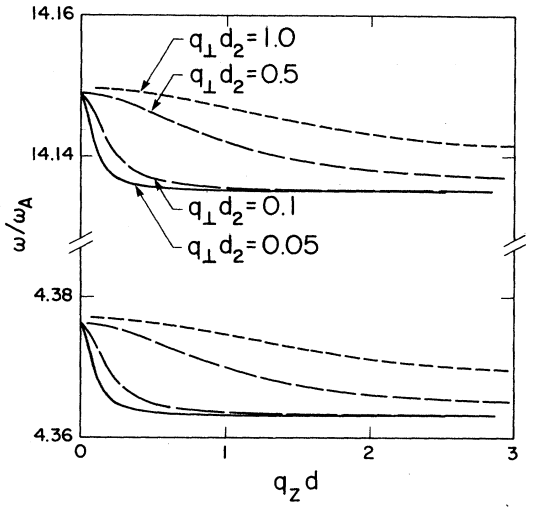

FIG. 15. Frequency of the "bulk-interface" modes as a function of $q_z d$ for an antiferromagnetic-paramagnetic superlattice. Several values of $q_\perp d_2$ have been selected. We have assumed that the antiferromagnetic and paramagnetic layers contain the same magnetic ions but that they occur in different concentrations. This means that the gyromagnetic ratio is the same for both layers. The thicknesses of the antiferromagnetic and paramagnetic layers are d_1 and d_2, respectively. The following parameters were used in the numerical calculation: $H_0 = 60$ kG, $H_E = 200$ kG, $H_A = 30$ kG, $M_0 = 0.2$ kG, and the magnetization in the paramagnetic layer is 0.07 kG at liquid-helium temperatures. The geometrical arrangement corresponds to $\mathbf{H}_0$ parallel to the axis of the superlattice and, for simplicity, to $d_1 = d_2$ (sample *SL3* in Ref. 13.)

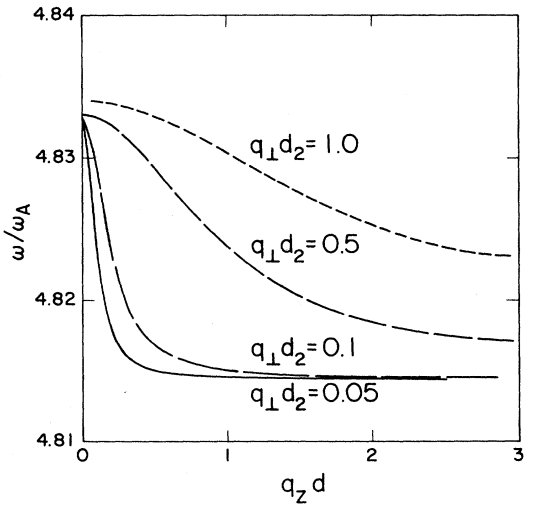

FIG. 16. Frequency of the "bulk-interface" modes occurring when the frequency lies in the narrow range $\omega_1' < \omega < \omega_2'$. Other geometrical features and numerical parameters as in Fig. 15.

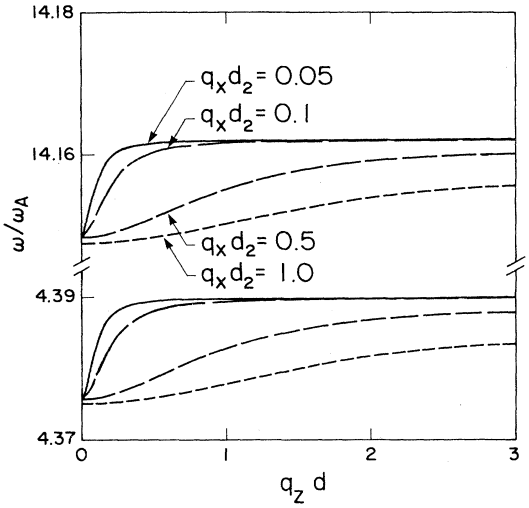

FIG. 17. Frequency of "bulk-interface" modes when $\mathbf{H}_0 \| \hat{x}$ and $q_y = 0$ as a function of $q_z d$ for several values of $q_x d_2$. Numerical parameters as in Fig. 15.

$H_0 = 60$ kG, for the example already mentioned, the frequencies of the allowed modes are given by $\omega/\omega_A \approx 4.39$ and ≈ 14.16 and do not appreciably change when $q_y d_2$ ranges from 0.05 to 1.0. These frequencies are approximately equal to σ_- and σ_+, respectively.

When $q_y = 0$, "pure bulk" modes appear if μ_1 and μ_2 are negative. The conditions on the frequency are identical to those of "pure bulk" modes when $\mathbf{H}_0$ is parallel to $\hat{z}$, namely, these magnetic excitations exist whenever there is overlap between the ranges $\omega_1 < \omega < \omega_2$ and $\omega_- < \omega < \sigma_-$. Ordinarily this implies that, if a mode exists, its frequency is approximately ω_1. For the material parameters used in our examples and $H_0 = 60$ kG, there is no overlap between the intervals $\omega_- < \omega < \sigma_-$ and

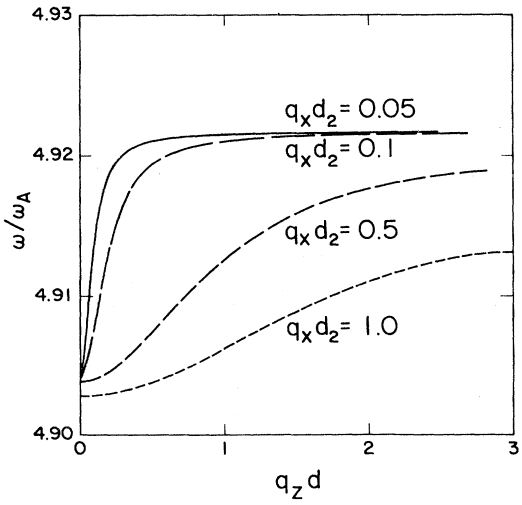

FIG. 18. Frequency in the range $\omega_1 < \omega < \omega_2$ of "bulk-interface" modes when $\mathbf{H}_0 \| \hat{x}$ and $q_y = 0$ as a function of $q_z d$ for several values of $q_x d_2$. Numerical parameters as in Fig. 15.

$\omega_1 < \omega < \omega_2$ and, hence, no "pure bulk" modes.

"Bulk-interface" modes occur in two cases: (i) $\mu_1 < 0, \mu_2 > 0$, and (ii) $\mu_1 > 0, \mu_2 < 0$. In case (i) the frequency of the modes is restricted to one of the ranges $\omega_- < \omega < \sigma_-$ and $\omega_+ < \omega < \sigma_+$ and must lie outside $\omega_1 < \omega < \omega_2$, this latter condition implying no practical limitation for paramagnetic layers. In case (ii), $\omega_1 < \omega < \omega_2$ and the frequency must lie in one of the three intervals $\omega < \omega_-$, $\sigma_- < \omega < \omega_+$, and $\omega > \sigma_+$. Thus, again, we expect a mode of approximate frequency ω_1. Figure 17 corresponds to case (i). It shows the frequencies of the two "bulk-interface" modes for $\mu_1 < 0$ and $\mu_2 > 0$ as functions of $q_z d$ for various values of $q_x d_2$. The numerical parameters are the same as those used in the previous examples. Figure 18 shows the frequency as a function of $q_z d$ for various values of $q_x d_2$ corresponding to case (ii).

B. Antiferromagnetic-nonmagnetic superlattices

The modes discussed above may also exist in semiconducting superlattices made of alternating antiferromagnetic (1) and nonmagnetic (2) layers. An example is $Cd_{1-x}Mn_xTe/CdTe$ ($x > 0.17$).

When $\mathbf{H}_0$ is parallel to the axis, $\hat{z}$, of the superlattice, $Q_1^2 = -\mu_1 q_1^2$ and $Q_2^2 = -q_1^2 (\mu_2 = 1)$. We see immediately that there can be no "pure bulk" modes. There are "bulk-interface" modes when $\mu_1 < 0$, i.e., for $\omega_- < \omega < \sigma_-$ or $\omega_+ < \omega < \sigma_+$. There are no "pure-interface" modes.

If $\mathbf{H}_0$ is parallel to the plane of the layers ($\mathbf{H}_0 \| \hat{x}$) we consider the two cases $q_x = 0$ and $q_y = 0$. When $q_x = 0$, $Q_{1,2}^2 = -q_y^2$ and we only obtain "pure-interface" modes. The quantity f defined in Eq. (3.15) must be negative in order for the right-hand side of Eq. (3.16) to be less than unity. In this case

$$f = 1 + \tfrac{1}{2}\omega_A^4 (\omega^2 - \sigma_+^2)^{-1} (\omega^2 - \sigma_-^2)^{-1} . \tag{4.1}$$

Now $f < 0$ requires ω to lie in the interval $\sigma_- < \omega < \sigma_+$. In addition,

$$(\omega^2 - \sigma_-^2)(\sigma_+^2 - \omega^2) < \tfrac{1}{2}\omega_A^4 \tag{4.2}$$

so that whenever

$$(\sigma_+^2 - \sigma_-^2)^2 > 2\omega_A^4 , \tag{4.3}$$

we obtain "pure-interface" modes when ω satisfies

$$\sigma_-^2 < \omega^2 < \tfrac{1}{2}(\sigma_+^2 + \sigma_-^2) - \tfrac{1}{2}[(\sigma_+^2 - \sigma_-^2)^2 - 2\omega_A^4]^{1/2} \tag{4.4}$$

or

$$\tfrac{1}{2}(\sigma_+^2 + \sigma_-^2) + \tfrac{1}{2}[(\sigma_+^2 - \sigma_-^2)^2 - 2\omega_A^4]^{1/2} < \omega^2 < \sigma_+^2 . \tag{4.5}$$

If the quantity under the radical is negative, i.e., if

$$H_0^2 = [(\omega_+ - \omega_-)/2\gamma]^2 \leq \frac{(\omega_A/\gamma)^4}{8(\omega_A/\gamma)^2 + 16(H_A^2 + 2H_A H_E)} , \tag{4.6}$$

then the inequality (4.2) is automatically satisfied and the

frequency of the "pure-interface" modes lies in the region $\sigma_- < \omega < \sigma_+$. For our example, (4.6) is satisfied for $H_0 < 0.33$ kG.

If $q_y = 0$, $Q_1^2 = -q_x^2/\mu_1$, and $Q_2^2 = -q_x^2$. There are no "pure bulk" modes. A simple analysis shows that there can be no "pure interface" waves. However, "bulk-interface" excitations occur when $\mu_1 < 0$, i.e., when $\omega_- < \omega < \sigma_-$ or $\omega_+ < \omega < \sigma_+$. These results are consistent with those obtained for a slab when the angle θ between $\mathbf{q}_\perp$ and $\mathbf{H}_0$ equals zero.

C. Ferromagnetic-nonmagnetic superlattices

We consider the case of a superlattice with alternating ferromagnetic (1) and nonmagnetic (2) layers. If $\mathbf{H}_0$ is parallel to $\hat{z}$, $Q_1^2 = -\mu_1 q_\perp^2$ and $Q_2^2 = -q_\perp^2$. We have here no "pure bulk" modes. There are "bulk-interface" modes when $\mu_1 < 0$ which requires $\omega_1' < \omega < \omega_2'$ since $\mu_1 = (\omega^2 - \omega_2'^2)(\omega^2 - \omega_1'^2)^{-1}$. We remark that unlike the paramagnetic case, ω_2' can now be significantly different from ω_1'. Equation (3.5) in this case reduces to

$$\cos(q_z d) = \cos[q_\perp d_1 (-\mu_1)^{1/2}]\cosh(q_\perp d_2) + \tfrac{1}{2}(1+\mu_1)(-\mu_1)^{-1/2}\sin[q_\perp d_1(-\mu_1)^{1/2}]\sinh(q_\perp d_2) \ . \tag{4.7}$$

There are "pure interface" modes if $\mu_1 > 0$ but this turns out to be inconsistent with Eq. (3.5). Therefore, only "bulk-interface" modes are possible in this geometry.

If $\mathbf{H}_0$ is parallel to $\hat{x}$ we consider first $q_x = 0$. Then $Q_{1,2}^2 = -q_y^2$ so that only "pure interface" modes exist. The dispersion relation is obtained from

$$\cos(q_z d) = \cosh(q_y d_1)\cosh(q_y d_2) + f \sinh(q_y d_1)\sinh(q_y d_2) \ , \tag{4.8}$$

where

$$f = (\mu_1^2 + 1 + 16\pi^2\chi_1^2)/(2\mu_1) = \left[\omega^2 - \frac{\omega_1^4 + \omega_2^4}{2\omega_1^2}\right](\omega^2 - \omega_2^2)^{-1} \ . \tag{4.9}$$

Equations (4.8) and (4.9) can be solved for ω as a function of q_z and q_y but its expression is not particularly useful. The range of frequencies accessible to the magnetostatic modes is restricted by Eqs. (4.8) and (4.9) to the values for which $\omega_2 < \omega < [(\omega_1^4 + \omega_2^4)/2\omega_1^2]^{1/2}$. An additional restriction follows from the requirement that the right-hand side of Eq. (4.8) must lie between -1 and 1.

For $q_y = 0$, $Q_1^2 = -q_x^2/\mu_1$, and $Q_2^2 = -q_x^2$. Therefore, there are no "pure bulk" modes. When $\mu_1 > 0$, use of

$$\cos(q_z d) = \cosh(q_x d_1 \mu_1^{-1/2})\cosh(q_x d_2) + \tfrac{1}{2}(1+\mu_1)\mu_1^{-1/2}\sinh(q_x d_1 \mu_1^{-1/2})\sinh(q_x d_2) \tag{4.10}$$

establishes the nonexistence of "pure interface" modes.

Finally, "bulk-interface" modes exist when $\mu_1 < 0$ which limits the frequencies to the range $\omega_1 < \omega < \omega_2$. There are, of course, possible additional restrictions arising from the consequence of Eq. (3.5) applied to the present conditions.

Our conclusions in relation to magnetic excitations in superlattices of DMS's are summarized as follows.

(1) In an antiferromagnetic-paramagnetic superlattice with $\mathbf{H}_0$ parallel to the growth axis there are three spin excitation branches, corresponding to "bulk-interface" modes. There are "pure bulk" modes but at magnetic fields of 60 kG they are absent using the parameters appropriate to $Cd_{0.89}Mn_{0.11}Te/Cd_{0.30}Mn_{0.70}Te$. Pure interface modes cannot occur in this geometry.

(2) When $\mathbf{H}_0$ is perpendicular to the axis of growth of the superlattice we distinguish between the cases $\theta = \pi/2$ ($q_x = 0$) and $\theta = 0$ ($q_y = 0$). In the first case, an antiferromagnetic-paramagnetic superlattice can only exhibit "pure interface" modes of which there are, for our example, three narrow branches at frequencies approximately independent of q_y. One of these occurs at $\omega \approx \omega_1 \approx \omega_2$. In the second case we can have only "bulk-interface" and "pure bulk" modes. There are three branches of "bulk-interface" modes. For the example chosen there are no "pure bulk" waves even though for other values of the magnetic field they may be present.

(3) In the case of antiferromagnetic-nonmagnetic superlattices the conclusions 1 and 2 are applicable except that there are no "pure bulk" modes at all.

(4) For ferromagnetic-nonmagnetic superlattices the conclusions are the same as for antiferromagnetic-nonmagnetic superlattices except that the frequency ranges are different.

We note that "pure bulk" modes are only possible in a superlattice when the allowed frequency intervals of "bulk" waves in the component layers overlap. This is expected because such waves can propagate in both media. When there is no overlap in the frequency ranges of slab modes, the spin waves propagate in one medium while their amplitudes decrease exponentially in the other. Such waves can be regarded as confined to the layer in which they propagate. This is in close analogy to the situation occurring in the propagation of optical phonons in superlattices.[16]

ACKNOWLEDGMENTS

This work was supported by the National Science Foundation (Grant No. DMR 85-20866), by the North Atlantic Treaty Organization (Research Grant No. 0759/87), and by Fonds National de la Recherche Scientifique (Belgium).

[1]R. W. Damon and J. R. Eshbach, J. Phys. Chem. Solids **19**, 308 (1961).
[2]R. E. Camley, T. S. Rahman, and D. L. Mills, Phys. Rev. B **27**, 261 (1983).
[3]P. Grünberg and K. Mika, Phys. Rev. B **27**, 2955 (1983).
[4]R. E. Camley and M. G. Cottam, Phys. Rev. B **35**, 189 (1987).
[5]M. Grimsditch, M. R. Khan, A. Kueny, and I. K. Schuller, Phys. Rev. Lett. **51**, 498 (1983).
[6]I. K. Schuller and M. Grimsditch, J. Appl. Phys. **55**, 2491 (1985).
[7]J. K. Furdyna, J. Vac. Sci. Technol. **21**, 220 (1982).
[8]J. K. Furdyna, J. Appl. Phys. **53**, 7637 (1982).
[9]J. K. Furdyna, J. Vac. Sci. Technol. **A4**, 2002 (1986).
[10]J. K. Furdyna and N. Samarth, J. Appl. Phys. **61**, 3526 (1987).
[11]A. K. Ramdas, J. Appl. Phys. **53**, 7649 (1982).
[12]S. Rodriguez and A. K. Ramdas, Pure Appl. Chem. **59**, 1269 (1987).
[13]E. K. Suh, D. U. Bartholomew, A. K. Ramdas, S. Rodriguez, S. Venugopalan, L. A. Kolodziejski, and R. L. Gunshor, Phys. Rev. B **36**, 4316 (1987).
[14]S. Rodriguez, A. Camacho, and L. Quiroga, Superlattices Microstructures **3**, 371 (1987).
[15]R. L. Stamps and R. E. Camley, J. Appl. Phys. **56**, 3437 (1984).
[16]See, e.g., A. K. Sood, J. Menendez, M. Cardona, and K. Ploog, Phys. Rev. Lett. **54**, 2115 (1985).